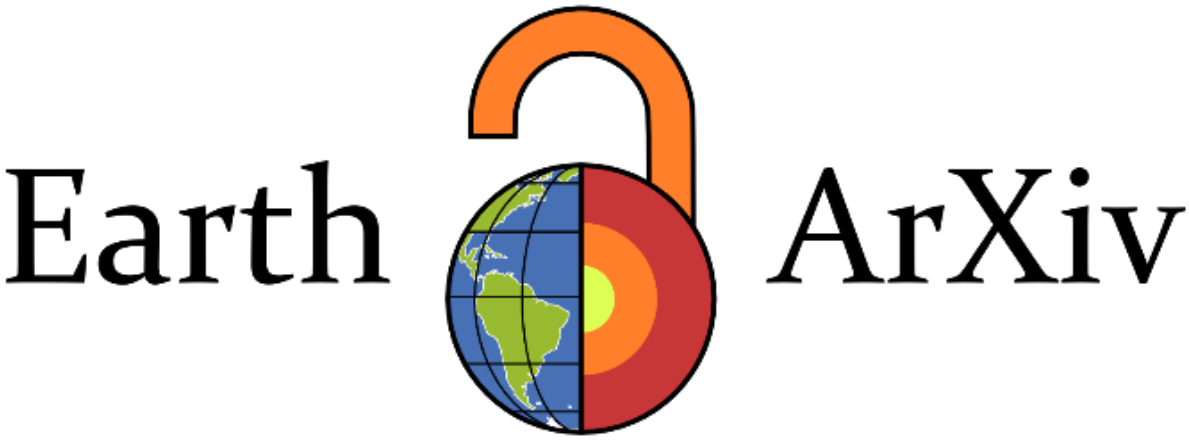

Large climate model ensembles reveal underdispersion in seasonal Atlantic tropical cyclone counts

E. L. Levin[a] G. A. Vecchi,[b,c] G. Villarini,[c,d]

[a] *Program in Atmospheric and Oceanic Sciences, Princeton University*

[b] *Department of Geosciences, Princeton University*

[c] *High Meadows Environmental Institute, Princeton University*

[d] *Department of Civil and Environmental Engineering, Princeton University*

Corresponding author: Emma Levin, emma.levin@princeton.edu

ABSTRACT: Seasonal Atlantic tropical cyclone (TC) counts are commonly modeled as a conditional Poisson process, implying that the distribution of possible seasonal outcomes—the range of TC counts that could plausibly occur in a given year—exhibits equidispersion for a given climate state, with its variance equal to its mean. This assumption underlies many statistical frameworks used for seasonal TC prediction and risk assessment, yet to the best of our knowledge has not been extensively tested directly. Using large ensembles from physics-based climate models (AM2.5-C360 and HiRAM) and a deep learning-based climate emulator (ACE2; Ai2 Climate Emulator version 2), we examine the distributional properties of seasonal TC counts in a controlled modeling framework. Across all models and years, we find that the ensemble distribution of within-season TC counts is systematically underdispersed, with ensemble variances smaller than their corresponding means. This behavior violates the equidispersion implied by a Poisson process and is consistent with a finite opportunity or binomial framework. This interpretation of TC genesis suggests that storms arise from a limited number of precursor disturbances whose likelihood of development depends on large-scale environmental conditions. We fit seasonal TC count distributions from a 1,000-member ACE2 ensemble to the Poisson and binomial distributions and find statistical evidence that the binomial formulation provides a better fit to TC count distributions. The Poisson assumption is not supported by current climate model simulations, given that simulated seasonal TC counts are more constrained than implied by traditional Poisson-based frameworks.

SIGNIFICANCE STATEMENT: Seasonal Atlantic tropical cyclone (TC) forecasts are critical for risk preparedness, energy planning, and insurance decision-making. Many statistical models used for these forecasts assume that TCs occur randomly, following a Poisson process. Leveraging unprecedentedly large ensembles from state-of-the-art physics-based and deep-learning climate models, we show that simulated seasonal TC counts systematically violate this assumption. Instead, TC counts are more constrained. This behavior is consistent with a physical picture in which TCs arise from a finite number of precursor disturbances ('seeds') whose likelihood of development depends on the large-scale environment. These results motivate more physically grounded statistical models for seasonal TC prediction.

1. Introduction

North Atlantic Tropical cyclones (TCs) can cause tens to hundreds of billions of dollars in damage annually in the United States, Americas, and Caribbean (Klotzbach et al. 2018), as well as mortality both coincident with the storm and for the years following (Young and Hsiang 2024). Understanding the controls on seasonal TC activity and developing accurate seasonal forecasts are an element of risk preparedness, energy planning, and insurance decision-making. Seasonal outlooks, issued prior to the climatological June through November TC season, predict the number of storms that will form throughout the season. These forecasts are generated using a range of modeling approaches, including dynamical climate models (e.g., Chen and Lin 2013; Murakami et al. 2016b, 2025; Vecchi et al. 2014; Zhao et al. 2010), deep learning (DL)–based weather prediction models (Zhang et al. 2025), and statistical or statistical–dynamical frameworks (e.g., Vecchi et al. 2011; Villarini et al. 2019). Seasonal TC predictions will necessarily be probabilistic in nature (Vecchi et al. 2014), so understanding both the expected TC activity and the plausible deviations from it are essential.

Statistical and statistical–dynamical approaches relate large-scale environmental conditions, such as sea surface temperature (SST), vertical wind shear, and atmospheric humidity, to seasonal Atlantic TC activity. Based on the statistical relationships of large-scale conditions to TCs, these approaches model the plausible distribution of seasonal TC counts conditioned on the large-scale environment for the given year. Early statistical studies (e.g., Gray 1984; Gray et al. 1992) used linear regression to link environmental predictors to TC counts, but such approaches can yield

non-integer predictions that are not physically meaningful for discrete storm counts. Subsequent developments innovatively addressed this limitation by explicitly modeling TC counts using discrete probability distributions. The canonical choice has been the Poisson distribution (e.g., Davis et al. 2015; Elsner and Jagger 2004, 2006; Jagger and Elsner 2010; Murakami et al. 2016a; Villarini et al. 2012), which provides a natural framework for count data. Additionally, Li et al. (2023) and Villarini et al. (2010) went to length to explore whether a Poisson model or Negative Binomial discrete model was better to fit the distribution of possible seasonal TC counts, and found that the Poisson model was better suited.

In the Poisson formulation, seasonal TC activity is assumed to arise from a Poisson process: storm occurrences within a season are treated as independent in time, each with a small probability of occurring within an infinitesimal interval, while their accumulation over the TC season yields a finite number of events. The process is fully characterized by a single rate parameter, representing the expected seasonal TC count, conditioned on the large-scale environmental conditions. Statistical and statistical–dynamical studies therefore seek to estimate this conditional rate parameter, typically via Poisson regression, by relating large-scale environmental conditions to the expected number of storms in a given season. A key implication of this assumption is equidispersion, meaning that the variance of the seasonal TC count distribution equals its mean.

The Poisson formulation is attractive due to its mathematical simplicity and minimal parameterization with one free parameter (i.e., seasonal rate parameter), and it is often motivated by viewing TC formation as the outcome of many random independent trials with a low probability of success at any given time (Blitzstein and Hwang 2014). However, the assumption that seasonal TC counts are equidispersed is a modeling convenience and statistical fit from several models (Villarini et al. 2010), rather than a physically derived constraint.

Several alternative discrete distributions have been proposed to represent seasonal TC counts. For example, Li et al. (2023) and Villarini et al. (2010) explored a negative binomial distribution, which allows for overdispersion relative to the Poisson model. In contrast, Vecchi et al. (2019) and Hsieh et al. (2020) propose that climatological TC activity be viewed through a binomial framework in which TC formation is viewed as a sequence of Bernoulli trials, with a finite number of precursor disturbances or seeds providing the number of trials for a given season. In this formulation, both seed frequency and the probability that a seed develops into a TC depend on the large-scale

environment, although the climate dependence of each is different. These alternative approaches imply fundamentally different dispersion properties of the seasonal TC count distribution. While the Poisson distribution is equidispersed, the negative binomial distribution is overdispersed (with the distribution variance larger than its mean), and the binomial distribution is underdispersed (with the distribution variance smaller than the mean) (Johnson et al. 2005). Dispersion plays a central role in seasonal TC prediction, as it governs the spread of possible outcomes for a given season. Differences in dispersion affect the probability of extremely active or inactive seasons, which correspond to outcomes with substantially different predictability and possibly distinct societal and economic consequences. Despite its importance, the equidispersion assumption underlying the Poisson formulation has rarely been tested directly, largely due to limited sample sizes in observations and traditional modeling frameworks.

A rigorous evaluation of the appropriate distribution for seasonal TC counts requires examining the distribution of simulated or forecasted counts across a large ensemble for a given season. In such ensembles, each member experiences identical large-scale environmental forcing, such as SST, but differs slightly in its initial conditions, representing a plausible realization of that season's TC activity. Confidence in quantifying dispersion and performing goodness-of-fit tests for discrete count distributions therefore requires a sufficiently large number of ensemble members, as these higher moments are less well constrained in typical dynamical model ensembles (order ten members).

Traditional seasonal TC prediction systems from physics-based numerical models are generally limited in ensemble size because of substantial computational costs. For example, the seasonal forecasting systems described in Murakami et al. (2025) and Zhang et al. (2025) employ approximately ten to fifteen and 20 ensemble members, respectively, and the AM2.5-C360 and HiRAM simulations used to examine multidecadal variability in Kortum et al. (2024) and Levin et al. (2026b) are limited to five to ten ensemble members. Such ensemble sizes are insufficient to robustly assess the distributional form and dispersion properties of seasonal TC counts.

Recent advances in DL–based weather and climate models provide an opportunity to overcome this limitation. Once trained, these models can be run efficiently at a fraction of the computational cost required by conventional dynamical models, enabling the generation of very large ensembles (e.g., Bi et al. 2023; Chen et al. 2023; Lam et al. 2023; Lang et al. 2024; Kochkov et al. 2024; Watt-

Meyer et al. 2025). These systems have been shown to realistically reproduce TC characteristics across subseasonal to interannual timescales (Chien et al. 2025) and recover a well-calibrated representation of internal variability of seasonal TC activity (Levin et al. 2026a). In this study, we leverage idealized and historical simulations from two atmosphere-only models developed at the Geophysical Fluid Dynamics Laboratory (GFDL), AM2.5-C360 and HiRAM, as well as a state-of-the-art DL–based climate emulator, ACE2, to generate large ensembles of seasonal TC counts. In particular, we use a 1,000-member ensemble from ACE2 to enable robust distributional and dispersion diagnostics.

This study addresses the following research question: Do seasonal Atlantic TC counts produced by state-of-the-art climate models satisfy the equidispersion implied by a Poisson process, or do they exhibit systematic departures consistent with alternative generative mechanisms? We further examine whether these properties are consistent across models with fundamentally different internal dynamics. In the following sections, we describe the models and experiments used in this analysis (Section 2), present evidence that seasonal Atlantic TC counts are underdispersed relative to Poisson expectations (Section 3), and discuss the implications of these findings for statistical TC prediction models, physical interpretations of TC genesis, and the use of large ensembles from AI-based climate emulators (Section 4).

2. Methods and data

a. Models and experiments

To simulate large ensembles of annual Atlantic TC seasons, we use a combination of global high-resolution dynamical atmospheric models and an DL-based climate and weather emulator. The dynamical models used in this study were developed at GFDL and implemented on the Princeton computing system (Chen and Lin 2013; Chan et al. 2021; Hsieh et al. 2020; Kortum et al. 2024; Levin et al. 2026b; Yang et al. 2021; Zhao et al. 2009): AM2.5-C360 and HiRAM.

We analyze a suite of idealized experiments with the dynamical models forced with distinct SST patterns. To generate large ensembles of TC activity under identical boundary forcing, each experiment is integrated for several decades, typically between 30 and 200 years. Each simulated year represents a plausible realization of TC activity under the prescribed SST pattern, since the boundary conditions remain fixed and the only source of variability arises from differences in

initial conditions. In this way, each experiment produces 30 to 200 ensemble members of seasonal TC activity. The experiments, summarized in Table 1, largely follow the designs used in previous studies (e.g., Hsieh et al. 2020, 2022). All experiments use prescribed monthly SST fields that remain fixed throughout the integration.

Each experiment builds on a control simulation in which both models are forced with the annual cycle of SSTs averaged over 1986 to 2005. This climatological cycle is repeated for 200 years in HiRAM and 100 years in AM2.5-C360 after a 10-year spin-up. The resulting long-term means represent the statistically steady-state climatological baselines for each model. TCs are tracked for every simulated year, and because the boundary conditions do not vary, each year is treated as an independent ensemble member characterizing TC activity under mean 1986–2005 conditions. Because the autocorrelation in aggregate of annual TC statistics is effectively zero, differences in ensemble members represent the result of internal atmospheric variability. Additional experiments apply perturbations to this baseline, including a uniform $+2K$ and $+4K$ SST warming and $-2K$ and $-4K$ SST cooling to the 1986-2005 climatology. We also analyze several experiments to represent isolated perturbations of greenhouse gas radiative forcing, where we double ($2\times CO_2$) carbon dioxide concentrations and multiply carbon dioxide concentrations by five ($p5\times CO2$) relative to the control experiment. Additionally, we explore an experiment where we both double atmospheric carbon dioxide concentrations and uniformly warm the climatological 1986-2005 SSTs by $+2K$ ($+2K$ $2\times CO_2$). These experiments are also described in Hsieh et al. (2020, 2022); Eusebi et al. (2025); Kortum et al. (2024); Levin et al. (2026b); Yang et al. (2021).

To investigate the influence of El Niño Southern Oscillation on Atlantic TC activity, we also explore El Niño and La Niña experiments, which are explained in Hsieh et al. (2022). In these cases, the prescribed SST annual cycles are derived from the strongest events between 1980 and 2015. The El Niño experiment (+Niño) uses the mean SST fields from nine years with Oceanic Niño Index (ONI) values greater than +1 (1982, 1986, 1987, 1991, 1994, 1997, 2002, 2009, 2015). The La Niña experiment (+Niña) uses the mean of seven years with ONI values below -1 (1988, 1995, 1998, 1999, 2007, 2010, 2011). Additionally, we analyze two additional experiments to highlight the contrast between El Niño and La Niña conditions. In the +Nina-Niño (+Nino-Niña) experiment are forced by subtracting the mean SST fields from the nine most active El Niño (seven most active La Niña) years between 1980 and 2015 from the seven most active La Niña (nine most

TABLE 1. List of idealized experiments used in this study, which are also used in Hsieh et al. (2020, 2022); Eusebi et al. (2025); Kortum et al. (2024); Levin et al. (2026b); Yang et al. (2021).

Experiment	Years (and models)	Description
CTL	100 (AM2.5-C360), 200 (HiRAM)	1986-2005 monthly climatological mean SSTs
+2K	50 (both)	Uniform SST warming
+4K	50 (HiRAM only)	Uniform SST warming
-2K	30 (HiRAM only)	Uniform SST cooling
-4K	30 (HiRAM only)	Uniform SST cooling
2×CO_2	50 (both)	CO_2 doubling
p5×CO_2	40 (HiRAM only)	×5 CO_2 increase
+2K & 2×CO_2	50 (both)	Uniform SST warming and CO_2 doubling
+Niño	50 (both)	SST annual cycles averaged over strong El Niño years
+Niña	50 (both)	SST annual cycles averaged over strong La Niña years
+Niño-Niña	50 (HiRAM only)	SST annual cycles averaged over strong El Niño years minus strong La Niña years
+Niña-Niño	50 (HiRAM only)	SST annual cycles averaged over strong La Niña years minus strong El Niño years

active El Niño) years during that time frame. All aforementioned simulations maintain a constant carbon dioxide concentration, with the exception of the $2\times CO_2$ experiments.

We also analyze multi-ensemble experiments with both models to represent historical TC seasons, described in detail in Levin et al. (2026b). For AM2.5-C360 we generated ten ensemble members, and for HiRAM we generated five ensemble members. Each member was forced with bias-corrected observed monthly SSTs (Chan et al. 2021) from the Hadley Centre Sea Ice and Sea Surface Temperature (HadISST) dataset for the period 1871–2021, and each was initialized with distinct atmospheric conditions while sharing identical SST forcing. Although ensembles of five or ten members are not sufficiently large to fit a discrete probability distribution to the outcomes, they allow us to evaluate the dispersion of simulated seasonal TC counts by examining the ratio of the ensemble variance to the ensemble mean.

In this study, we employ the DL-based Ai2 Climate Emulator version 2 (ACE2; Watt-Meyer et al. (2025)) trained on ERA5 reanalysis (Hersbach et al. 2020) to perform huge ensemble annual simulations of several Atlantic TC seasons. The model is forced by observed HadISST SSTs (Schneider et al. 2013) and by annually varying greenhouse gas concentrations. Previous studies have demonstrated that ACE2 can reproduce subseasonal and interannaul global TC behavior (Chien et al. 2025) and recover a well-calibrated representation of internal seasonal Atlantic TC

variability (Levin et al. 2026a), motivating our use of the model to generate large ensembles of Atlantic TC seasons to investigate the range of plausible outcomes. We generate 1,000 ensemble members for the continuous period 2005-2020 and for the anomalously inactive 1982 Atlantic TC season following the methods of Levin et al. (2026a).

b. Data and storm tracking

For the historical record of observed Atlantic TC counts from 1878 to 2024, we utilize the adjusted dataset developed using the methods of Landsea et al. (2010) and assessed in Villarini et al. (2011), where we require that storm maximum wind speeds must exceed 17 m s^{-1} for at least 48 hours.

We follow the approach described in Levin et al. (2026b) to track TCs and seed disturbances in both dynamical models. Specifically, we apply the tracking algorithm of Harris et al. (2016), which identifies candidate storms based on local minima in sea level pressure and applies additional thresholds on vorticity, warm-core structure, wind speed, and duration. Consistent with Villarini et al. (2011), we require all identified TCs to have a minimum lifetime of 72 hours. To track TCs in the ACE2 DL model, we adopt a similar approach following Chien et al. (2025) and Levin et al. (2026b). In this case, we use the TempestExtremes algorithm (Ullrich and Zarzycki 2017), which also detects systems based on local minima in sea level pressure and applies additional constraints on wind speed, duration, location, and warm-core structure.

c. Theoretical TC proxy

As in Levin et al. (2026b) and Levin et al. (2026a), we employ Hsieh et al. (2020)'s probabilistic framework, which decomposes annual TC counts into a precursor seed disturbance phase followed by the phase during which the seed develops into a full TC. Thus, the annual number of Atlantic TCs is assumed to follow a binomial distribution:

$$N_{TC} \sim \text{binom}(N_s, P), \tag{1}$$

where N_s is the number of seeds and P is the probability that a seed disturbance transitions into a fully developed TC. Consequently, the expected seasonal count of Atlantic TCs N_{TC}, is given by

$$N_{TC} = N_s \times P. \tag{2}$$

In this study, we evaluate the seed–probability framework by using explicitly tracked seed counts to estimate N_s, although the seed proxy developed by Hsieh et al. (2020) has developed a climate-conditioned expectation for seed frequency. Additionally, the probability that a seed develops into a TC (P) is parameterized as a function of the large-scale environmental conditions ($P(\Lambda)$):

$$P \approx P(\Lambda) = \frac{1}{1 + (\Lambda_0/\Lambda)^{1/\gamma}}, \tag{3}$$

where $\Lambda_0 = 0.014$ and $\gamma = -0.9$ are constant dimensionless fitting parameters, and

$$\Lambda = \frac{\nu_s \cdot \chi}{PI}, \tag{4}$$

is the ventilation index defined by Tang and Emanuel (2010) and Tang and Emanuel (2012), measuring the degree to which entrainment of low entropy air can limit the storm's intensity. ν_s is vertical wind shear, PI is potential intensity, and χ is moist entropy deficit. As in Levin et al. (2026b), We compute the mean Atlantic basin $P(\Lambda)$ over 10–30°N. Following the methodology of Hsieh et al. (2020) and Vecchi et al. (2019), we compute the proxy during the climatologically most active portion of the season, June–November.

3. Results

a. Unprecedentedly large ACE2 historical ensemble

We display the seasonal TC count distributions simulated from the 1,000-member ACE2 historical ensemble in Figure 1, adapted from Figure 2 of Levin et al. (2026a). Overall, the ACE2 ensemble exhibits strong calibration to the observed record across multiple metrics. The Q–Q calibration diagnostic (Figure 1b) closely follows the 1:1 line, indicating that the observed TC counts verify approximately uniformly across the ensemble distributions. This suggests that, in a probabilistic sense, the model is well calibrated to the observed record. Consistent with the results

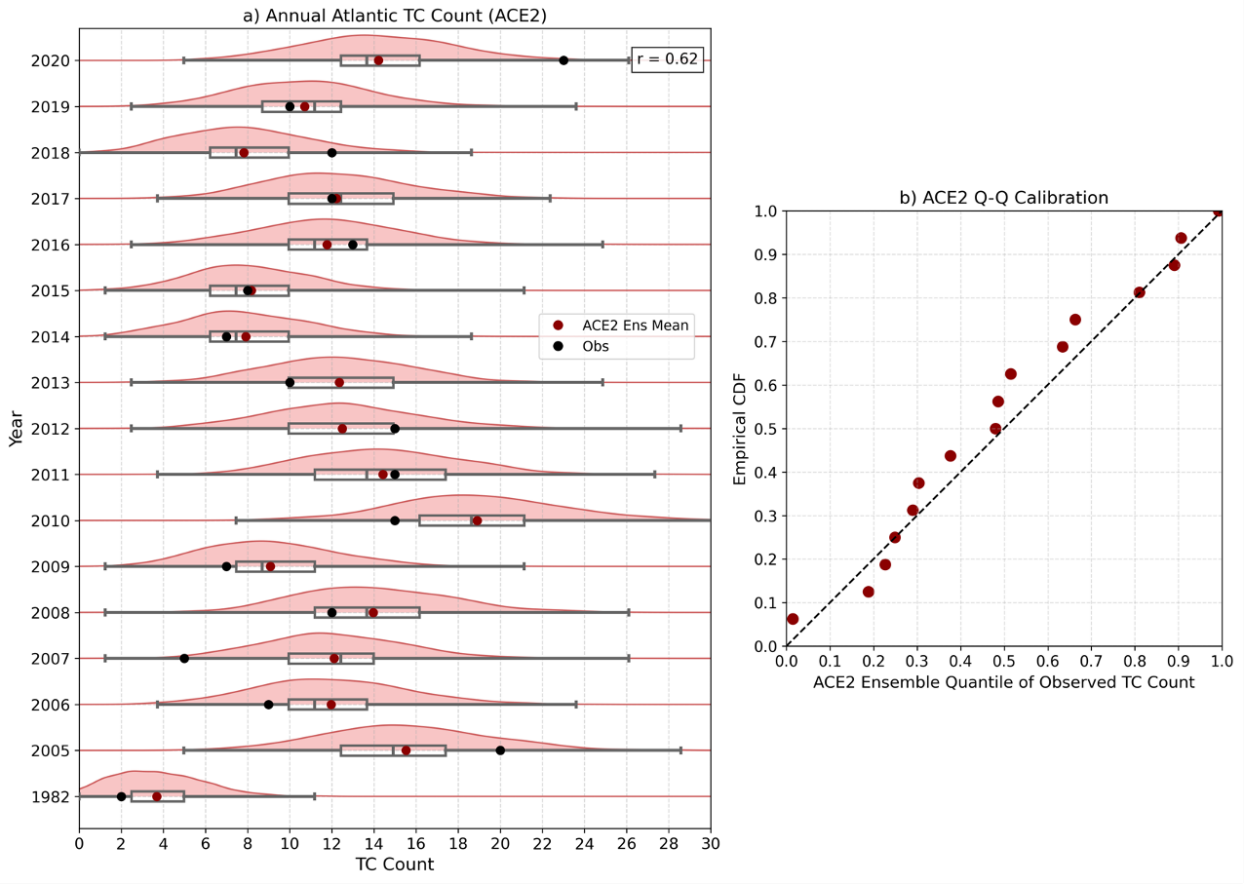

FIG. 1. a) The simulated historical observed SST-forced ACE2 1,000-member ensemble distribution of annual Atlantic TC counts for 1982 and 2005–2020, shown in red using kernel density estimate (KDE) probability density functions, with the corresponding box-and-whisker plots overlaid in gray for each year. The whiskers denote the ensemble minimum and maximum values, the box edges represent the 25th and 75th percentiles, and the center line indicates the median of the distribution. The red dot represents the ensemble mean, and the black dot represents the observed TC count computed using the methods of Landsea et al. (2010). The correlation between the annual ensemble-mean TC count and the observed counts is shown in the upper-right corner. b) Quantile–quantile (Q–Q) calibration diagnostic of ACE2 over the 17 verification years, where each point represents the empirical cumulative distribution of the observed TC count within the corresponding ensemble distribution. A well-calibrated ensemble is indicated by alignment with the black dashed 1:1 line. This figure has been adapted from Levin et al. (2026a).

of the Q–Q plot, the observed TC count lies within the ensemble range for all years considered, and falls within the interquartile range (25th–75th percentile) for eight of the seventeen seasons.

The correlation between the ensemble-mean and observed TC counts ($r = 0.62$) further indicates that the model captures a substantial portion of the interannual variability. This retrospective skill is comparable to that of other dynamical and statistical methods (e.g., Vecchi et al. 2014; Zhao et al. 2009).

The shape and spread of the seasonal distributions also exhibit systematic structure. Most seasons (eleven out of seventeen) display positive skewness, indicating a tendency toward relatively more inactive outcomes with a long tail of more active realizations. Fewer seasons are approximately symmetric (four seasons) or negatively skewed (two seasons). The total ensemble range (maximum minus minimum count) varies considerably across years, from eleven storms in 1982 to 26 storms in 2012, highlighting substantial interannual differences in the spread of plausible outcomes.

Despite the overall model calibration, there are notable seasons in which the observed TC count lies in the tails of the ensemble distribution. For example, during the relatively inactive 2007 season (five observed TCs), the ACE2 ensemble distribution is centered around approximately twelve TCs, placing the observation in the lower tail. Conversely, the 2020 season was extremely active (23 observed TCs), while the ensemble distribution is centered near fourteen TCs, with the observed count verifying near the 99.5th percentile (Levin et al. 2026a). This result suggest that the 2020 season reflected a combination of subseasonal variability and intrinsic unpredictability that even well-calibrated, state-of-the-art models may fail to capture. Refer to Levin et al. (2026a) for a well-calibrated distribution of seasonal TC counts for the 2020 season. Finally, while the kernel density estimates (KDEs) of Figure 1 provide a qualitative visualization of the ensemble distributions, they are not well suited for quantifying dispersion. In the following section, we therefore formally assess the dispersion properties of the ACE2 seasonal TC count distributions and compare them with those from physics-based climate models.

b. Dispersion of simulated conditional TC counts across models

We examine the relationship between the ensemble mean and variance of seasonal Atlantic TC counts under identical boundary forcing in Figures 2a and 2c across a suite of models and experiments. For each season, we compute the ensemble mean and ensemble variance of TC counts subjected to the same prescribed SST forcing, with each point in these figures representing the mean–variance pair associated with a single season.

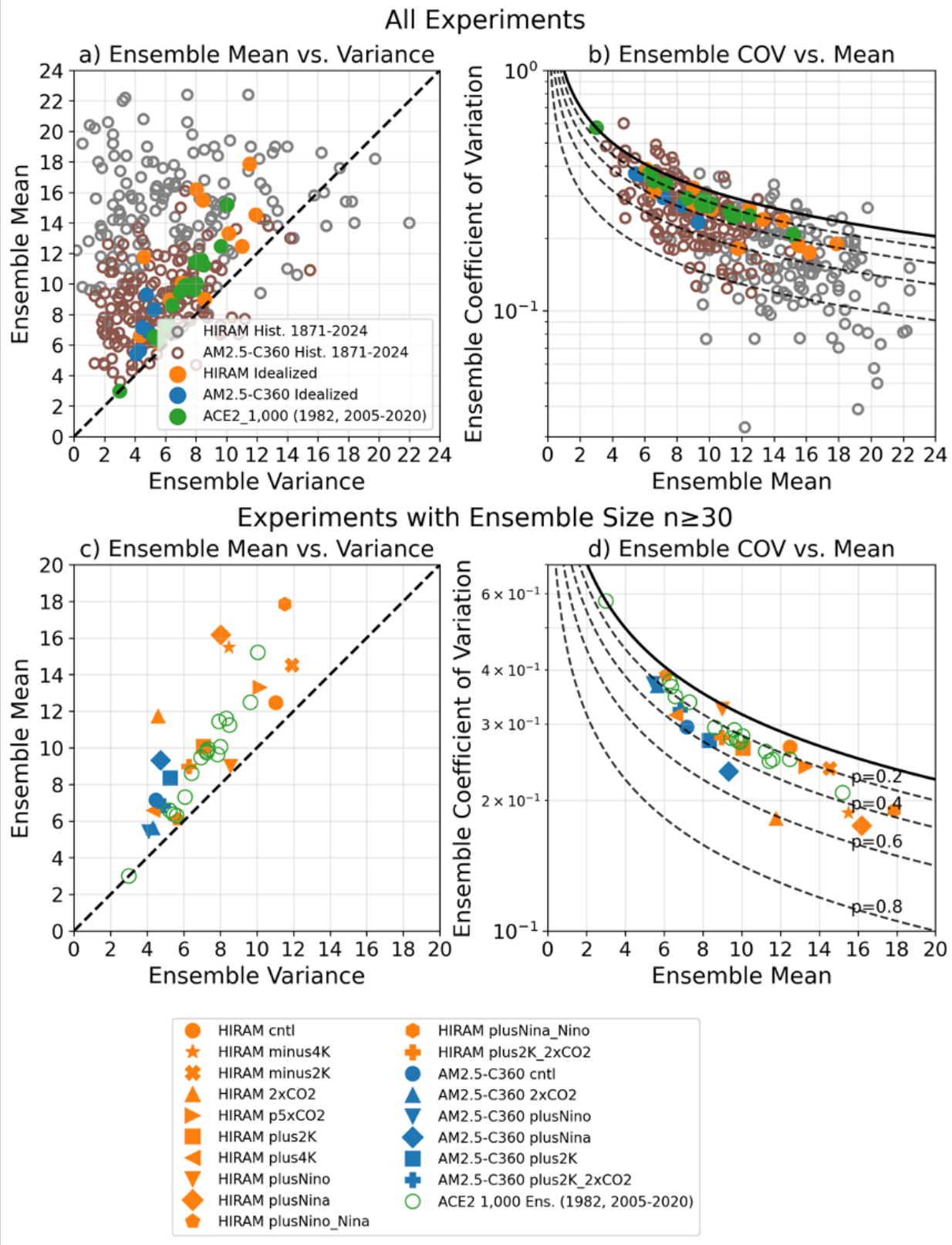
All Experiments
a) Ensemble Mean vs. Variance
b) Ensemble COV vs. Mean
Ensemble Mean
Ensemble Variance
Ensemble Coefficient of Variation
HIRAM Hist. 1871-2024
AM2.5-C360 Hist. 1871-2024
HIRAM Idealized
AM2.5-C360 Idealized
ACE2_1,000 (1982, 2005-2020)
Experiments with Ensemble Size n≥30
c) Ensemble Mean vs. Variance
d) Ensemble COV vs. Mean
p=0.2
p=0.4
p=0.6
p=0.8
HIRAM cntl
HIRAM minus4K
HIRAM minus2K
HIRAM 2xCO2
HIRAM p5xCO2
HIRAM plus2K
HIRAM plus4K
HIRAM plusNino
HIRAM plusNina
HIRAM plusNino_Nina
HIRAM plusNina_Nino
HIRAM plus2K_2xCO2
AM2.5-C360 cntl
AM2.5-C360 2xCO2
AM2.5-C360 plusNino
AM2.5-C360 plusNina
AM2.5-C360 plus2K
AM2.5-C360 plus2K_2xCO2
ACE2 1,000 Ens. (1982, 2005-2020)

FIG. 2. a) Relationship between the ensemble mean and variance of seasonal Atlantic TC counts under identical SST forcing, shown across a suite of models and experiments. Each point corresponds to a single season or experiment and represents the variance–mean pair computed from the ensemble distribution of TC counts. Brown-outlined (gray-outlined) points denote historical AM2.5-C360 (HiRAM) simulations forced with observed SSTs, blue (orange) points indicate idealized experiments from AM2.5-C360 (HiRAM), and green points represent the historical 1,000-member ACE2 ensemble. The black dashed line shows the 1:1 relationship, corresponding to equidispersion. Points below (above) the line indicate underdispersion (overdispersion). b) Relationship between the ensemble mean and the coefficient of variation of seasonal TC counts, using the same models, experiments, and color scheme as in panel (a). The solid black curve indicates the Poisson expectation, $COV = 1/\sqrt{\mu}$, while the dashed black curves indicate the Binomial expectation, $COV = \sqrt{\frac{1-p}{\mu}}$, where p=0.2, 0.4, 0.6, and 0.6, labeled in panel d). c,d) Same as panels (a) and (b), respectively, but excluding the smaller-ensemble historical AM2.5-C360 and HiRAM simulations. Idealized experiments are distinguished by marker shape. Experiments shared across both models (i.e. the 'cntl' experiment) have the same marker shape across both models.

Across all models and experiments, including both historical and idealized simulations, seasonal TC counts are systematically underdispersed. This behavior is evident from the fact that most points lie above the 1:1 line, indicating that the ensemble variance is smaller than the ensemble mean for most seasons. The only points lying below the 1:1 line are from the smaller ensemble sized experiments of HiRAM (five members) and AM2.5-C360 (ten members), where the sample variance is less likely to represent the true underlying variance due to the small sample size. Even for those historical experiments, the vast majority of points for HiRAM (141/154) and AM2.5-C360 (145/154) lie above the 1:1 line. Idealized simulations from AM2.5-C360 and HiRAM (Figures 2a and 2c) exhibit this pattern for all experiments. The 1,000-member historical ensemble generated using ACE2 (Figures 2a and 2c) also displays pronounced underdispersion, with sixteen of the seventeen examined seasons exhibiting variances lower than their corresponding means, and none showing overdispersion. The remaining season, 1982, is approximately equidispersed, with both the mean and variance near three TCs. This season is exceptionally inactive relative to typical TC seasons and represents an outlier within the ensemble. Taken together across several state-of-the-art climate models with different underlying dynamics, seasonal Atlantic TC activity

violates the equidispersion property of the Poisson distribution and provide clear evidence against a simple conditional Poisson process description of seasonal TC counts in these models.

We further find that the relationship between ensemble mean and variance becomes more tightly organized as ensemble size increases. For large ensembles with more than 30 members, as in the ACE2 simulations and AM2.5-C360 and HiRAM idealized experiments shown in Figure 2c, the mean–variance pairs cluster closely around a well-defined curve and remain within a small distance of the 1:1 line. In contrast, the AM2.5-C360 and HiRAM historical ensembles, which contain substantially fewer members (five to ten members), exhibit greater scatter, with some seasons lying close to the 1:1 line and others deviating more strongly. This behavior is consistent with sampling variability in the estimation of variance from small ensembles and demonstrates that larger ensemble sizes yield more robust and stable estimates of the dispersion properties of seasonal TC counts.

In addition to examining the relationship between the ensemble mean and variance, we analyze how the ensemble coefficient of variation (COV) varies with the ensemble mean of seasonal Atlantic TC counts in Figures 2b and 2d. The COV is defined as

$$COV = \frac{\sigma}{\mu}, \tag{5}$$

where σ is the ensemble standard deviation and μ is the ensemble mean. The COV is a dimensionless measure of relative dispersion that quantifies the magnitude of variability normalized by the mean. Smaller values of COV indicate lower relative dispersion, while larger values indicate greater relative variability. Examining how COV varies with μ therefore provides insight into how relative model uncertainty changes for seasons with different levels of simulated TC activity.

The expected relationship between COV and μ differs between common discrete count models. For a Poisson distribution, the mean and variance are equal, such that $\mu = \sigma^2 = \lambda$, where λ is the rate parameter. In this case,

$$COV_{\text{Poisson}} = \frac{\sigma}{\mu} = \frac{\sqrt{\mu}}{\mu} = \frac{1}{\sqrt{\mu}}, \tag{6}$$

implying that the coefficient of variation decreases with increasing mean solely due to counting statistics. A decreasing COV with increasing μ is therefore expected under a Poisson process.

For a binomial distribution describing n independent Bernoulli trials with success probability p, the mean and variance are given by $\mu = np$ and $\sigma^2 = np(1-p)$. The corresponding COV is

$$COV_{\text{Binomial}} = \frac{\sigma}{\mu} = \frac{\sqrt{np(1-p)}}{np} = \sqrt{\frac{1-p}{\mu}}. \tag{7}$$

Both Poisson and binomial models therefore predict that COV decreases with increasing μ and scales as $1/\sqrt{\mu}$. However, the binomial distribution includes an additional multiplicative factor of $\sqrt{1-p}$, which suppresses COV relative to the Poisson expectation for $0 < p < 1$. As a result, binomial processes predict systematically smaller coefficients of variation than Poisson processes at comparable mean values.

We examine the relationship between ensemble COV and ensemble mean μ of seasonal Atlantic TC counts under identical boundary forcing across a suite of models and experiments in Figures 2b and 2d. For each season, COV and μ are computed from the distribution of TC counts across ensemble members subjected to the same prescribed SST forcing. Each point therefore represents a COV–μ pair associated with a single season.

Across all models and experiments, including both historical and idealized simulations, the ensemble COV decreases with increasing ensemble mean: the relative model uncertainty is smaller in seasons with larger simulated activity. While this decreasing trend alone does not distinguish between Poisson and binomial processes, we find that the majority of COV–μ pairs lie below the Poisson expectation given by $COV = 1/\sqrt{\mu}$. Instead, these points fall within the range predicted by a binomial framework, as illustrated by the curves corresponding to $COV = \sqrt{(1-p)/\mu}$ for representative values of $p = 0.2, 0.4, 0.6$, and 0.8. This behavior is evident in both the physics-based AM2.5-C360 and HiRAM simulations and is particularly clear in the 1,000-member historical ensemble generated using the ACE2 model, for which all seasons except 1982 fall below the Poisson curve.

Taken together, the systematically reduced COV relative to the Poisson expectation provides further evidence against a simple Poisson process description of seasonal TC counts. Instead, these results are consistent with a finite-opportunity or Bernoulli trial framework, in which TC formation is governed by a limited number of precursor disturbances and environment-dependent conversion probabilities. Furthermore, the clustering of points from the larger ensemble simulations within

the binomial expectation curves for p between 0.2 and 0.4 in Figure 2d suggests that this range represents a plausible set of effective seed-to-TC conversion probabilities across the modeled climate states considered here.

c. Goodness-of-fit tests for 1,000 member ACE2 ensemble

Next, we examine the seasonal Atlantic TC count distributional properties of the 1,000-member ACE2 historical ensemble. The large ensemble size allows robust statistical inference that is not possible for conventional seasonal prediction systems, which typically include only a few dozen members. We analyze ensemble distributions for each season in the continuous period from 2005 to 2020 and 1982, with summary statistics for each season reported in Table 2. Each row in the table represents properties of the seasonal TC count distribution across the 1,000 ensemble members.

As shown in Figure 2, all sixteen seasons in the 2005-2020 period exhibit ensemble variances that are smaller than their corresponding means, indicating systematic underdispersion. Variance-to-mean ratios range from 0.69 to 0.84 for these years, while coefficients of variation range from 0.21 to 0.38. The strongest deviation from equidispersion between 2005-2020 occurs in 2010, which has the lowest variance-to-mean ratio and coefficient of variation, while 2018 is closest to equidispersed behavior during this period. This consistent underdispersion demonstrates that the equidispersion property implied by a Poisson process is not supported by the ACE2 ensemble distributions during the 2005-2020 period.

To further assess whether the ACE2 simulated Atlantic seasonal TC count distributions are consistent with a Poisson process, we conduct Monte Carlo experiments. For each season, we generate 10,000 synthetic ensembles by drawing 1,000 samples 10,000 times from a Poisson distribution with rate parameter equal to the ACE2 ensemble-mean TC count for that season. For each synthetic ensemble, we compute the sample variance, yielding a distribution of variances expected under Poisson sampling variability at the given mean.

We illustrate the results for two representative seasons, 2010 and 2018, which span the range of dispersion characteristics in the ACE2 ensemble during the 2005–2020 period (Figure 3). Monte Carlo Poisson simulation results for all seasons are shown in Figure S1. Under the Poisson assumption, the ACE2 ensemble variance for a given season should fall within the distribution of variances generated by these Monte Carlo simulations.

TABLE 2. Characteristics of the seasonal Atlantic TC count distributions derived from a 1,000-member ensemble of the ACE2 historical simulation forced with observed seasonal SSTs. For each season, ensemble mean, variance, variance-to-mean ratio, and COV are shown. Akaike Information Criterion (AIC) scores are computed by fitting the ensemble TC counts to Poisson and binomial distributions using maximum likelihood estimation and method of moments. We do not include a Binomial fit for the 1982 season, since the estimate of the number of trials $\hat{n}$ in the method of moments estimation is negative, rendering the estimation unphysical. The quantity Δ AIC is defined as the AIC of the binomial fit minus that of the Poisson fit, such that negative values indicate a preferred binomial formulation.

Year	Mean	Variance	Variance/Mean	COV	AIC Poisson	AIC Binomial	Δ AIC
1982	2.96	2.97	1.00	0.58	3863.8	–	–
2005	12.5	9.7	0.78	0.25	5129.7	5100.7	-29.0
2006	9.6	7.9	0.82	0.29	4909.9	4892.3	-17.6
2007	9.7	7.3	0.75	0.28	4851.3	4814.6	-36.7
2008	11.2	8.5	0.76	0.26	5009.4	4975.9	-33.5
2009	7.3	6.1	0.84	0.34	4636.1	4622.2	-13.9
2010	15.2	10.1	0.66	0.21	5217.1	5144.8	-72.3
2011	11.6	8.3	0.72	0.25	4999.1	4951.9	-47.2
2012	10.1	8.0	0.79	0.28	4931.1	4909.5	-21.6
2013	9.9	7.3	0.74	0.27	4874.9	4834.3	-40.6
2014	6.3	5.5	0.87	0.37	4526.5	4516.8	-9.7
2015	6.6	5.2	0.79	0.35	4494.1	4472.8	-21.3
2016	9.5	7.0	0.74	0.28	4817.0	4775.4	-41.6
2017	9.8	7.3	0.74	0.28	4850.7	4810.9	-39.8
2018	6.3	5.6	0.89	0.38	4550.3	4545.9	-4.4
2019	8.6	6.4	0.74	0.29	4730.0	4693.3	-36.7
2020	11.4	7.9	0.69	0.25	4964.2	4906.6	-57.6

Instead, we find that the ACE2 ensemble variance lies in the extreme left tail of the Monte Carlo distributions for most seasons, indicating substantially reduced ensemble spread relative to Poisson expectations. This behavior is summarized in Figure 3c, which shows the percentile rank of the ACE2 ensemble variance relative to the corresponding Poisson-based variance distribution for each season. For thirteen of the seventeen seasons analyzed, the ACE2 ensemble variance falls below the minimum variance produced by the Poisson simulations. With the exception of 1982, for the remaining three seasons, the ACE2 ensemble variance lies below the 5th percentile of the Monte Carlo distribution.

These results provide strong evidence that the ACE2 seasonal TC count distributions are systematically underdispersed relative to a Poisson process. In particular, the observed variances are not merely smaller than the Poisson expectation, but fall outside the range of sampling variability expected under Poisson statistics for most seasons. This indicates that the discrepancy cannot be attributed to finite-sample effects, but instead reflects a fundamental deviation from Poisson behavior in the simulated TC count distributions.

Finally, the large ensemble size allows direct likelihood-based comparison of Poisson and binomial models using the Akaike Information Criterion (AIC). For the historical simulated ACE2 seasons, we fit the 1,000 ensemble TC counts to both distributions. The Poisson model is fit by setting the rate parameter equal to the sample mean, corresponding to the maximum likelihood and method of moments estimate. For the binomial model, parameters are estimated using the method of moments, with the conversion probability given by $\hat{p} = 1 - s^2/\bar{x}$ and the number of trials given by $\hat{n} = \bar{x}/\hat{p}$, where s is the sample standard deviation and $\bar{x}$ is the sample mean. For each fitted distribution, we compute the AIC,

$$AIC = 2k - 2\ln(\hat{L}), \tag{8}$$

where k is the number of free parameters in the model (one for Poisson, two for Binomial), and $\hat{L}$ is the maximum likelihood of the model. Thus, the AIC quantifies the trade-off between goodness of fit and model complexity, allowing objective comparison of competing distributional models for ensemble TC counts. Lower AIC values indicate a closer approximation to the underlying data-generating process. AIC values for the ACE2 simulated seasons are listed in Table 2.

Across all ACE2 simulated seasons between 2005 and 2020, the binomial model yields a lower AIC than the Poisson one, indicating superior explanatory power for the ensemble TC count distributions using a binomial distribution. While this does not rule out other underdispersed count models for seasonal Atlantic TC count distributions, such as the COM-Poisson or Poisson-binomial distributions, it demonstrates that the Poisson assumption is not supported by the 2005-2020 ACE2 ensemble data, whereas a Bernoulli-trials framework provides a substantially better description of the simulated seasonal Atlantic TC counts.

Although all seasons from 2005–2020 in the ACE2 historical ensemble exhibit clear underdispersion, characterized by ensemble variances below the 5th percentile of Poisson expectations (Fig. 3)

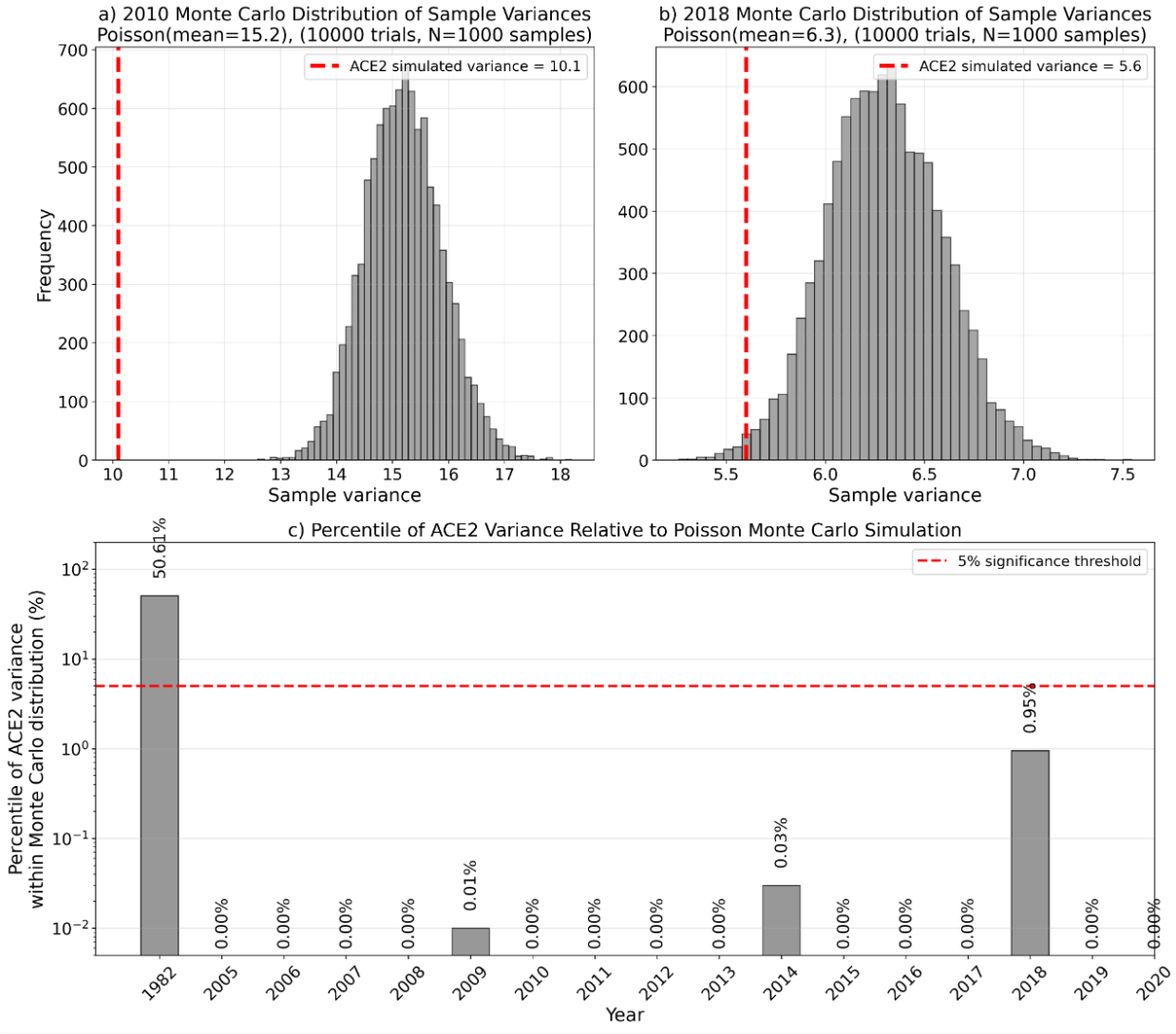

FIG. 3. Monte Carlo assessment of seasonal TC counts Poisson assumption using the 1,000-member ACE2 ensemble. Panels (a) and (b): For each year (2010 and 2018, respectively), 10,000 Monte Carlo realizations are generated by drawing 1,000 samples from a Poisson distribution with mean equal to the ACE2 ensemble mean for that season, thereby simulating the ensemble variance that would be expected if seasonal TC counts followed a Poisson process. Gray histograms show the resulting distribution of sample variances; the vertical red dashed line marks ACE2 ensemble variance. Monte Carlo distributions for all remaining years (1982, 2005–2020) are provided in Figure S1. Panel (c): Percentile of the ACE2 ensemble variance within its corresponding Monte Carlo variance distribution, indicating how frequently a Poisson process would produce a variance as low as or lower than that observed, shown for all available years on a logarithmic scale. The red dashed horizontal line marks the 5% significance threshold. With the exception of 1982, the ACE2 ensemble variance falls below the 5th percentile in every year, confirming that under-dispersion relative to Poisson is a consistent feature of the ensemble across the full record.

and superior goodness-of-fit to a binomial distribution relative to a Poisson distribution based on AIC (Table 2), the 1982 season represents a notable exception. As shown in Table 2, the simulated TC count distribution for 1982 is approximately equidispersed, with its mean and variance nearly equal. Consistent with this finding, the ensemble variance lies near the 51st percentile of the Monte Carlo Poisson variance distribution, indicating no clear deviation from Poisson variability for this particular season. Furthermore, because the ensemble variance slightly exceeds the mean, the binomial distribution cannot be meaningfully fit: the implied estimate of the number of trials $\hat{n}$ becomes negative, rendering the parameterization unphysical. Correspondingly, the Poisson distribution yields the lowest AIC score for 1982 among all candidate models across all years considered, further supporting the interpretation that this season is consistent with equidispersion.

We interpret 1982 as an outlier within both the observational record and the modeled ensemble. According to the observational dataset of Landsea et al. (2010), 1982 is the least active Atlantic TC season in the satellite era, with only two observed storms. Such an anomalously inactive environment likely limits the ability to robustly characterize the underlying distribution of TC counts, as the small number of events constrains the range of possible variability. Additionally, because the minimum possible seasonal TC count is zero, when the distribution mean of the simulated distribution is very low, the distribution variance approaches zero as well, making dispersion properties difficult to diagnose. In this regime, the distinction between different discrete distributions becomes less pronounced, and equidispersion can arise naturally due to the low count.

Importantly, the presence of other relatively inactive seasons within the ACE2 analysis period, such as 2007, which also exhibits low observed activity of five storms, does not lead to similar behavior. These seasons continue to display underdispersion and favor a binomial representation over a Poisson distribution. This indicates that low activity alone does not imply consistency with Poisson statistics. Taken together, these results suggest that the near-equidispersed behavior in 1982 reflects the uniquely extreme and unfavorable environmental conditions of that season, rather than a breakdown of the broader conclusions. Across all other seasons analyzed, the ACE2 1,000-member ensembles consistently support the conclusion that seasonal TC counts are not well described by a Poisson process, but are more appropriately represented by a binomial distribution.

d. Physical basis for the binomial TC framework

The results presented thus far provide strong evidence against describing seasonal TC counts as a Poisson process. They instead motivate consideration of alternative generative frameworks in which TC formation is more constrained than implied by purely random arrivals. Here, we present empirical support for a finite-opportunity or binomial framework for tropical cyclogenesis, following the conceptual model proposed by Hsieh et al. (2020); in this framework, seasonal TC counts are interpreted as the number of successes arising from a finite number of precursor disturbances or seeds, with the probability of each seed developing into a TC governed by large-scale environmental conditions.

Previous studies have demonstrated the utility of binomial-type frameworks for describing TC variability across a range of timescales, including the annual cycle (Yang et al. 2021) and longer-term climate variability and idealized experiments (Hsieh et al. 2020, 2022, 2023; Vecchi et al. 2019), especially in the Atlantic basin (Levin et al. 2026b). Building on this work, we explicitly examine tracked TC seeds and an independent proxy for the environmental conversion probability, as described in Section 2, in historical atmosphere-only simulations from AM2.5-C360 and HiRAM.

Figure 4 illustrates the ensemble-mean relationships among simulated seasonal TC counts, the binomial proxy defined as the product of seed count and conversion probability (Seeds $\times P(\Lambda)$), the individual components of this proxy, and the relationship between seed count and conversion probability. Across both models, we find moderate to strong positive correlations between seasonal TC counts and each component of the binomial framework. In AM2.5-C360, TC counts are more strongly correlated with seed count than with conversion probability ($r = 0.73$ versus $r = 0.53$), whereas in HiRAM the opposite is true, with TC counts more strongly correlated with conversion probability than with seed count ($r = 0.83$ versus $r = 0.62$). Despite these differences, the correlation between the full binomial proxy (Seeds $\times P(\Lambda)$) and simulated TC counts is strongly positive in both models ($r = 0.76$ for AM2.5-C360 and $r = 0.81$ for HiRAM), indicating that the combined influence of seeds and environmental favorability provides a robust predictor of seasonal TC activity.

We further note that seed count and conversion probability are not independent variables, but instead exhibit moderate positive covariance in both models ($r = 0.43$ for AM2.5-C360 and $r = 0.54$

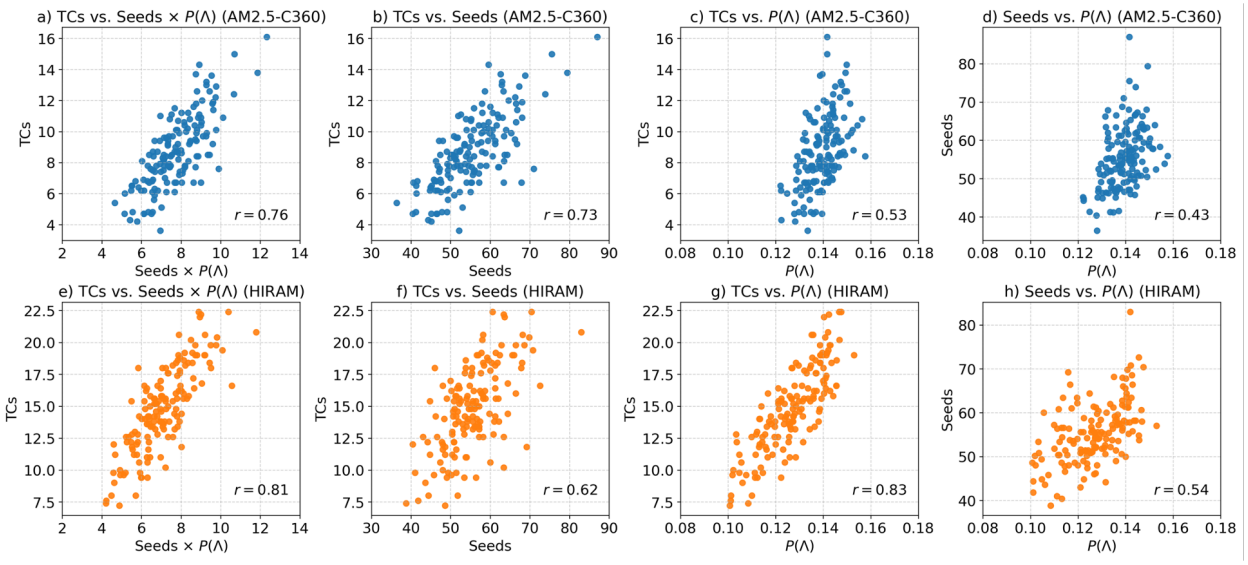

Fig. 4. Scatter plots illustrating relationships between ensemble-mean TC counts, precursor disturbances, and conversion probability in historical atmosphere-only simulations forced with observed SSTs during 1871–2021. Panels (a,e) show ensemble-mean TC count versus the ensemble-mean approximated TC count, defined as the product of seed count and parametrized conversion probability (Seeds $\times P(\Lambda)$). Panels (b,f) show ensemble-mean TC count versus ensemble-mean seed count. Panels (c,g) show ensemble-mean TC count versus ensemble-mean parametrized conversion probability $P(\Lambda)$. Panels (d,h) show ensemble-mean seed count versus ensemble-mean parametrized conversion probability. Top panels correspond to the AM2.5-C360 model (blue), and bottom panels correspond to the HiRAM model (orange). Correlation coefficients are reported in the lower-right corner of each panel.

for HiRAM), consistent with previous findings (Levin et al. 2026b). This covariance suggests that environmental conditions conducive to TC formation may simultaneously influence both the number of precursor disturbances and their likelihood of development. Taken together, the relationships shown in Figure 4 are consistent with a generative picture in which seasonal TC counts arise from a finite number of seeds whose conversion probability depends on the large-scale environment, rather than from an unbounded Poisson process. However, in spite of this colinearity, seeds and genesis probability together provide better explanatory power of seasonal TC frequency, as has also been found in other contexts and models (Hsieh et al. 2020; Levin et al. 2026b; Vecchi et al. 2019; Yang et al. 2021): seasonal TC frequency arises from the finite probability genesis from a finite set of trials (seeds), each of which are climate dependent.

4. Discussion and conclusions

This study provides the first systematic test of the Poisson equidispersion assumption for seasonal Atlantic TC counts using large state-of-the-art climate model ensembles. By leveraging ensembles from both physics-based atmosphere-only models (AM2.5-C360 and HiRAM) and a 1,000-member ensemble generated by a DL–based climate emulator (ACE2), we are able to robustly characterize the distributional properties of seasonal TC counts under identical boundary forcing across multiple modeling frameworks. The analysis here indicates that seasonal TC frequency should be best thought of as a multi-stage process consistent with some recent physically-based arguments (Hsieh et al. 2020).

Several independent lines of evidence consistently support a finite-opportunity interpretation of TC genesis rather than a Poisson process. First, seasonal TC count distributions are systematically underdispersed, with ensemble variances smaller than ensemble means across nearly all seasons, experiments, and models examined. Second, the relationship between the coefficient of variation and the ensemble mean deviates from the Poisson expectation, with relative uncertainty decreasing more rapidly in more active simulated seasons than predicted by a Poisson process. Third, Monte Carlo experiments demonstrate that the observed ensemble variances are inconsistent with those expected under Poisson randomness. Fourth, likelihood-based comparisons using AIC show that a binomial distribution provides a superior fit to the seasonal TC count distributions from the 1,000-member ACE2 ensemble in nearly all seasons examined. Finally, diagnostics based on precursor disturbances and environmental conversion probability provide physical support for a binomial framework, consistent with previous studies (Hsieh et al. 2020; Levin et al. 2026b; Sugi et al. 2020; Vecchi et al. 2019; Yang et al. 2021).

These results, implying that simulated TC activity is more constrained than implied by a Poisson process have important implications:

- **Statistical modeling of TCs**: Poisson-based formulations may systematically overestimate uncertainty and misrepresent dispersion structure for seasonal Atlantic TC count distributions, especially in active seasons. Alternative underdispersed count models, including binomial, Poisson-binomial, or related formulations, may provide more physically consistent representations of seasonal TC variability.

- **TC forecasting**: The decline in relative ensemble spread during simulated active seasons (Figures 2b and 2d) implies that models are inherently more confident when environmental conditions strongly favor TC formation. This behavior has direct relevance for how uncertainty is communicated in seasonal outlooks, particularly for high-impact seasons. This may arise, in part, due to the modest colinearity between seed frequency and genesis likelihood (Levin et al. 2026b).

- **Physical interpretability**: The results reinforce the view that TC counts are controlled by the joint behavior of precursor disturbances (seeds) and environmental conversion probability, rather than by purely random arrivals. Additionally, the binomial framework offers a physical mechanism for why the TC count distribution coefficient of variation decreases with the distribution mean (Figures 2b and 2d), thus the models exhibit less uncertainty for more active seasons:

  1. For a binomial distribution, the COV is given by

$$\mathrm{COV} = \sqrt{\frac{1-p}{np}}.$$

     When the conversion probability p is held fixed, the COV decreases as $1/\sqrt{n}$. Consequently, when a basin experiences a large number of trials or seed disturbances, the relative spread in total TC counts across the ensemble is reduced. This behavior reflects a law-of-large-numbers effect: as the number of trials increases, the total number of successes becomes more tightly constrained and more consistent across realizations. Thus, in seasons with abundant seeds (n), the realized TC counts are intrinsically less variable.

  2. A complementary interpretation involves variations in the conversion probability p. As shown in Figures 4c and 4g, more active seasons are associated with enhanced environmental favorability, reflected in higher values of $P(\Lambda)$. As p increases, the numerator of the COV expression ($\sqrt{1-p}$) decreases, driving the TC count distribution toward increasingly deterministic outcomes. For example, a conversion probability of $p = 0.99$ yields a substantially smaller COV than $p = 0.5$. In highly favorable

environments, in addition to more seeds being present, nearly every viable seed develops into a storm, leading to stronger agreement across ensemble members in their simulated TC activity.

- **Role of AI models**: This study highlights the unique role of AI-based climate models in enabling statistical diagnostics that were previously infeasible. The ability to generate ensembles with thousands of members allows robust estimation of dispersion properties and formal goodness-of-fit testing for discrete count distributions, opening new opportunities to re-examine long-standing statistical assumptions in climate science. At the same time, interpreting these AI-driven results relies critically on a strong understanding of the underlying physical processes governing storms, the large-scale climate, and their interactions. Together, this highlights the importance of integrating physical insight with advanced statistical and computational approaches.

Several caveats are important to note. Our analysis is conducted within a controlled modeling framework, whereas the observational record provides only a single realization of each TC season, precluding direct empirical estimation of observed seasonal count distributions. Furthermore, interannual variability in observed TC counts reflects not only stochastic variability within a given climate state, but also systematic changes in the climate forcing across years, such as SSTs. As such, variability in observed TC counts can be decomposed as

$$\sigma^2_{\text{total}} = \sigma^2_{\text{noise}} + \sigma^2_{\text{climate}}, \tag{9}$$

where σ^2_{total} is the total interannual variance in seasonal TC counts, σ^2_{noise} represents intrinsic stochastic variability within a fixed climate state for a given season, and $\sigma^2_{\text{climate}}$ represents variability due to changes in the large-scale climate (e.g., SST patterns). In our controlled modeling framework, large ensembles allow direct estimation of σ^2_{noise} by holding the climate state fixed. In contrast, the observational record conflates these two components, making it difficult to directly assess the intrinsic dispersion of seasonal TC counts.

To partially address this limitation and quantify a measure of dispersion in the observed TC record, we estimate the *conditional dispersion* of the observed seasonal TC counts, Y_t^{obs}, for year t, after accounting for the influence of climate and SST, denoted by X_t. We define the conditional

dispersion as

$$\phi_{\text{obs}|X} \approx \frac{\text{Var}(Y^{\text{obs}} \mid X)}{\text{E}(Y^{\text{obs}} \mid X)}, \tag{10}$$

where $\phi_{\text{obs}|X}$ quantifies the dispersion of TC counts conditional on the climate state. Values $\phi_{\text{obs}|X} < 1$ indicate underdispersion, $\phi_{\text{obs}|X} = 1$ indicates equidispersion, and $\phi_{\text{obs}|X} > 1$ indicates overdispersion.

Because only a single observed count is available for each year, we approximate this quantity using historical atmosphere-only simulations forced with observed SSTs. For each year t, we define the residual

$$e_t = Y_t^{\text{obs}} - \hat{\mu}_t, \tag{11}$$

where $\hat{\mu}_t$ is the ensemble-mean TC count from the corresponding model simulation for that year. To account for mean bias between the model and observations, we apply a single multiplicative scaling factor to the model output, such that $\hat{\mu}_t$ represents a bias-corrected estimate of the climate-conditioned mean TC count.

We then estimate the conditional variance from the residuals as

$$\widehat{\text{Var}}(Y^{\text{obs}} \mid X) = \frac{1}{N-b} \sum_{t=1}^{N} e_t^2, \tag{12}$$

where N is the number of years and $b = 1$ is the number of fitted mean parameters (the multiplicative scaling factor). The conditional mean is estimated as the average ensemble mean TC count across all years of the model simulation:

$$\widehat{\text{E}}(Y^{\text{obs}} \mid X) = \frac{1}{N} \sum_{t=1}^{N} \hat{\mu}_t. \tag{13}$$

Substituting these estimates into Equation 10 yields an estimate of the conditional dispersion of the observational record.

We apply this methodology using observed TC counts derived following Landsea et al. (2010) for the period 1878–2024, and historical simulations from ACE2, HiRAM, and AM2.5-C360 forced by observed SSTs (Section 2). Results are shown in Table 3. We compute dispersion both including

TABLE 3. Conditional dispersion (Equation 10) computed by comparing observed TC counts to historical model simulations forced with observed SSTs, using all years and all years excluding 2020.

Model	All years	Excluding 2020
ACE2 (1982, 2005–2020)	1.17	0.82
HiRAM (1878–2024)	1.25	1.09
AM2.5-C360 (1878–2024)	1.10	0.97

all years and excluding 2020, which has been identified as a high-leverage outlier for TC counts (Levin et al. 2026a).

When all years are included, the conditional residuals are modestly overdispersed across all three models. However, excluding 2020 leads to a systematic reduction in dispersion across all models. For ACE2 and AM2.5-C360, the dispersion becomes less than or near unity, suggesting conditional underdispersion or near-equidispersion. In contrast, HiRAM remains slightly overdispersed. These results highlight the disproportionate influence of the 2020 season. As an extremely active year, 2020 lies in the far tail of the ACE2 ensemble distribution and outside the spread of the smaller dynamical model ensembles. As a result, it contributes strongly to the residual variance and inflates the estimated dispersion. The sensitivity of $\phi_{\text{obs}|X}$ to the inclusion of a single extreme season underscores the limited sample size of the observational record and the challenges of estimating dispersion from a single realization per year.

More broadly, these results suggest that the dispersion characteristics of the observational record remain uncertain when conditioned on climate. Differences across models, as well as sensitivity to the inclusion of specific years, indicate that estimates of $\phi_{\text{obs}|X}$ are influenced not only by intrinsic variability but also by model-dependent representations of the climate-conditioned mean. In particular, residual variance reflects both true stochastic variability and errors in the estimated mean state; imperfect representation of the climate-conditioned mean can artificially inflate dispersion estimates. In contrast, large ensemble modeling frameworks provide a more direct and robust means of quantifying dispersion, as they allow explicit separation of stochastic variability from climate-driven changes in the mean. The consistency of underdispersion identified across physics-based models, idealized experiments, and the ACE2 DL emulator, independent of observational constraints, suggests that underdispersion is a robust feature of the modeled TC genesis process across several modeling frameworks. The observational analysis presented here should therefore

be interpreted as a complementary, but inherently limited, attempt to assess dispersion in the real world.

As another caveat, this study focuses exclusively on seasonal Atlantic TC counts, a basin for which Poisson-based statistical models have been widely applied (e.g., Davis et al. 2015; Elsner and Jagger 2004, 2006; Jagger and Elsner 2010; Murakami et al. 2016a; Villarini et al. 2012). Preliminary analysis suggests that qualitatively similar underdispersion in the ensemble spread of modeled seasonal TC activity is also present in the western North Pacific; however, a quantitative assessment of whether Poisson or binomial frameworks provide an appropriate description of seasonal TC counts in that basin is beyond the scope of this study. Future work should therefore examine dispersion properties across additional basins and evaluate the suitability of alternative discrete count models, particularly given the use of Poisson formulations for TC counts in regions such as the Pacific (McDonnell and Holbrook 2004).

Finally, our results do not assess model accuracy or forecast skill. Several seasons, including 2007 and 2020, lie in the extreme tails of the model-simulated TC count distributions (Figure 1), indicating that accurate prediction of individual seasons remains challenging. As discussed in Levin et al. (2026a), and expected from the intrinsically probabilistic nature of seasonal TC information (e.g., Vecchi and Villarini 2014; Vecchi et al. 2014), such discrepancies may arise from the intrinsic unpredictability of subseasonal atmospheric variability rather than deficiencies in the model representation of TC genesis itself. Our findings instead clarify how climate models generate distributions of possible seasonal outcomes and provide a physically grounded interpretation of their dispersion properties.

Overall, this work demonstrates the value of combining physics-based and DL–based climate models to rigorously test foundational statistical assumptions. By showing that seasonal TC counts in climate models are underdispersed and more constrained than implied by Poisson randomness, we motivate the development of more physically grounded statistical frameworks for seasonal TC prediction and risk assessment.

Acknowledgments. We thank Libby Barnes, Greg Hakim, and Peter Huybers for helpful discussion and comments, and we thank Spencer Clark at Ai2, Mu-Ting Chien at Boston University, and Colm Talbot and Mattie Niznik at Princeton Research Computing for their assistance in running the ACE2 model. This work has been supported by the Carbon Mitigation Initiative at Princeton University, funded by BP. E.L. was supported by the National Science Foundation Graduate Research Fellowship. This work was funded, in part, by the Heising-Simons Foundation Grant 2023-4720. The simulations were performed on computational resources managed and supported by Princeton Research Computing, a consortium of groups including the Princeton Institute for Computational Science and Engineering, the Office of Information Technology's High Performance Computing Center, and the Visualization Laboratory at Princeton University.

Data availability statement. Source code of the HiRAM model is available from `https://www.gfdl.noaa.gov/hiram-quickstart`, and the source code of the ACE2 model is available from `https://github.com/ai2cm/ace`. The code to run one year's 1,000-member ensemble and process the output, and track TCs is available at `https://github.com/emmalevin/ACE2_1000`. TC track data and monthly mean environmental conditions generated from the ACE2 1,000 member ensemble are available at the Zenodo repository: `https://doi.org/10.5281/zenodo.19456833`.

References

Bi, K., L. Xie, H. Zhang, X. Chen, X. Gu, and Q. Tian, 2023: Accurate medium-range global weather forecasting with 3d neural networks. *Nature*, **619 (7970)**, 533–538, https://doi.org/10.1038/s41586-023-06185-3.

Blitzstein, J. K., and J. Hwang, 2014: *Introduction to Probability*. 1st ed., Texts in Statistical Science, Chapman and Hall/CRC, Boca Raton, FL.

Chan, D., G. A. Vecchi, W. Yang, and P. Huybers, 2021: Improved simulation of 19th- and 20th-century north atlantic hurricane frequency after correcting historical sea surface temperatures. *Science Advances*, **7 (26)**, eabg6931, https://doi.org/10.1126/sciadv.abg6931.

Chen, J.-H., and S.-J. Lin, 2013: Seasonal predictions of tropical cyclones using a 25-km-resolution general circulation model. *Journal of Climate*, **26 (2)**, 531–543, https://doi.org/10.1175/JCLI-D-12-00061.1.

Chen, L., X. Zhong, F. Zhang, Y. Cheng, Y. Xu, Y. Qi, and H. Li, 2023: Fuxi: A cascade machine learning forecasting system for 15-day global weather forecast. *npj Climate and Atmospheric Science*, **6 (1)**, 190, https://doi.org/10.1038/s41612-023-00512-1.

Chien, M.-T., E. A. Barnes, and E. D. Maloney, 2025: Modulation of tropical cyclogenesis on subseasonal-to-interannual timescales in the deep-learning climate emulator ace2. *Machine Learning: Earth*, **1 (1)**, 015 008, https://doi.org/10.1088/3049-4753/adfd61.

Davis, K., X. Zeng, and E. A. Ritchie, 2015: A new statistical model for predicting seasonal north atlantic hurricane activity. *Weather and Forecasting*, **30 (3)**, 633–647, https://doi.org/10.1175/WAF-D-14-00156.1.

Elsner, J. B., and T. H. Jagger, 2004: A hierarchical bayesian approach to seasonal hurricane modeling. *Journal of Climate*, **17 (14)**, 2813–2824, https://doi.org/10.1175/1520-0442(2004)017⟨2813:AHBATS⟩2.0.CO;2.

Elsner, J. B., and T. H. Jagger, 2006: Prediction models for annual u.s. hurricane counts. *Journal of Climate*, **19 (12)**, 2935–2952, https://doi.org/10.1175/JCLI3729.1.

Eusebi, R., W. Yang, G. A. Vecchi, and S. Fueglistaler, 2025: Statistical modeling of north atlantic hurricane frequency and the impact and role of patterned warming. *Journal of Climate*, **38 (19)**, 5391–5410, https://doi.org/10.1175/JCLI-D-24-0647.1.

Gray, W. M., 1984: Atlantic seasonal hurricane frequency. part ii: Forecasting its variability. *Monthly Weather Review*, **112 (9)**, 1669–1683, https://doi.org/10.1175/1520-0493(1984)112⟨1669:ASHFPI⟩2.0.CO;2.

Gray, W. M., C. W. Landsea, J. Mielke, Paul W., and K. J. Berry, 1992: Predicting atlantic seasonal hurricane activity 6–11 months in advance. *Weather and Forecasting*, **7 (3)**, 440–455, https://doi.org/10.1175/1520-0434(1992)007⟨0440:PASHAM⟩2.0.CO;2.

Harris, L. M., S.-J. Lin, and C. Tu, 2016: High-resolution climate simulations using GFDL HiRAM with a stretched global grid. *Journal of Climate*, **29 (11)**, 4293–4314, https://doi.org/10.1175/JCLI-D-15-0389.1.

Hersbach, H., and Coauthors, 2020: The ERA5 global reanalysis. **146 (730)**, 1999–2049, https://doi.org/10.1002/qj.3803.

Hsieh, T.-L., G. A. Vecchi, W. Yang, I. M. Held, and S. T. Garner, 2020: Large-scale control on the frequency of tropical cyclones and seeds: a consistent relationship across a hierarchy of global atmospheric models. *Climate Dynamics*, **55 (11)**, 3177–3196, https://doi.org/10.1007/s00382-020-05446-5.

Hsieh, T.-L., W. Yang, G. A. Vecchi, and M. Zhao, 2022: Model spread in the tropical cyclone frequency and seed propensity index across global warming and enso-like perturbations. *Geophysical Research Letters*, **49 (7)**, e2021GL097 157, https://doi.org/10.1029/2021GL097157.

Hsieh, T.-L., B. Zhang, W. Yang, G. A. Vecchi, M. Zhao, B. J. Soden, and C. Wang, 2023: The influence of large-scale radiation anomalies on tropical cyclone frequency. *Journal of Climate*, **36 (16)**, 5431–5441, https://doi.org/10.1175/JCLI-D-22-0449.1.

Jagger, T. H., and J. B. Elsner, 2010: A consensus model for seasonal hurricane prediction. *Journal of Climate*, **23 (22)**, 6100–6113, https://doi.org/10.1175/2010JCLI3686.1.

Johnson, N. L., A. W. Kemp, and S. Kotz, 2005: *Univariate Discrete Distributions*. 3rd ed., Wiley Series in Probability and Statistics, Wiley, Hoboken, NJ.

Klotzbach, P. J., S. G. Bowen, R. Pielke, and M. Bell, 2018: Continental u.s. hurricane landfall frequency and associated damage: Observations and future risks. *Bulletin of the American Meteorological Society*, **99 (7)**, 1359–1376, https://doi.org/10.1175/BAMS-D-17-0184.1.

Kochkov, D., and Coauthors, 2024: Neural general circulation models for weather and climate. *Nature*, **632 (8027)**, 1060–1066, https://doi.org/10.1038/s41586-024-07744-y.

Kortum, G., G. A. Vecchi, T.-L. Hsieh, and W. Yang, 2024: Influence of weather and climate on multidecadal trends in atlantic hurricane genesis and tracks. *Journal of Climate*, **37 (5)**, 1501–1522, https://doi.org/10.1175/JCLI-D-23-0088.1.

Lam, R., and Coauthors, 2023: Learning skillful medium-range global weather forecasting. *Science*, **382 (6677)**, 1416–1421, https://doi.org/10.1126/science.adi2336.

Landsea, C. W., G. A. Vecchi, L. Bengtsson, and T. R. Knutson, 2010: Impact of duration thresholds on atlantic tropical cyclone counts. https://doi.org/10.1175/2009JCLI3034.1.

Lang, S., and Coauthors, 2024: AIFS: ECMWF's data-driven forecasting system. URL https://arxiv.org/abs/2406.01465, arXiv preprint, https://doi.org/10.48550/arXiv.2406.01465, 2406.01465.

Levin, E. L., M.-T. Chien, E. Barnes, H. He, G. A. Vecchi, and W. Yang, 2026a: On the seasonal predictability of the 2020 north atlantic tropical cyclone season. https://doi.org/10.31223/X5CN1R.

Levin, E. L., G. A. Vecchi, and W. Yang, 2026b: Influence of sea surface temperature patterns and mean warming on past and future atlantic tropical cyclone activity. *Journal of Climate*, **39 (10)**, 3735–3758, https://doi.org/10.1175/JCLI-D-25-0635.1.

Li, X., J. Ghosh, and G. Villarini, 2023: Bayesian negative binomial regression model with unobserved covariates for predicting the frequency of north atlantic tropical storms. *Journal of Applied Statistics*, **50 (9)**, 2014–2035, https://doi.org/10.1080/02664763.2022.2063266.

McDonnell, K. A., and N. J. Holbrook, 2004: A poisson regression model approach to predicting tropical cyclogenesis in the australian/southwest pacific ocean region using the soi and saturated equivalent potential temperature gradient as predictors. *Geophysical Research Letters*, **31 (20)**, L20 101, https://doi.org/10.1029/2004GL020843.

Murakami, H., T. L. Delworth, N. C. Johnson, F. Lu, C. E. McHugh, and L. Jia, 2025: Seasonal forecasts of tropical cyclones using GFDL SPEAR and HiFLOR-s. *Journal of Climate*, **38 (9)**, 3601–3620, https://doi.org/10.1175/JCLI-D-24-0356.1.

Murakami, H., G. Villarini, G. A. Vecchi, W. Zhang, and R. Gudgel, 2016a: Statistical–dynamical seasonal forecast of north atlantic and u.s. landfalling tropical cyclones using the high-resolution gfdl flor coupled model. *Monthly Weather Review*, **144 (6)**, 2217–2236, https://doi.org/10.1175/MWR-D-15-0308.1.

Murakami, H., and Coauthors, 2016b: Seasonal forecasts of major hurricanes and landfalling tropical cyclones using a high-resolution gfdl coupled climate model. *Journal of Climate*, **29 (22)**, 7977–7994, https://doi.org/10.1175/JCLI-D-16-0233.1.

Schneider, D. P., C. Deser, J. Fasullo, and K. E. Trenberth, 2013: Climate data guide spurs discovery and understanding. *Eos, Transactions American Geophysical Union*, **94 (13)**, 121–122, https://doi.org/10.1002/2013EO130001.

Sugi, M., Y. Yamada, K. Yoshida, R. Mizuta, M. Nakano, C. Kodama, and M. Satoh, 2020: Future changes in the global frequency of tropical cyclone seeds. *SOLA*, **16**, 70-74, https://doi.org/10.2151/sola.2020012.

Tang, B., and K. Emanuel, 2010: Midlevel ventilation's constraint on tropical cyclone intensity. *Journal of the Atmospheric Sciences*, **67 (6)**, 1817-1830, https://doi.org/10.1175/2010JAS3318.1.

Tang, B., and K. Emanuel, 2012: A ventilation index for tropical cyclones. *Bulletin of the American Meteorological Society*, **93 (12)**, 1901-1915, https://doi.org/10.1175/BAMSD1100165.1.

Ullrich, P. A., and C. M. Zarzycki, 2017: TempestExtremes: a framework for scale-insensitive pointwise feature tracking on unstructured grids. *Geoscientific Model Development*, **10 (3)**, 1069–1090, https://doi.org/10.5194/gmd-10-1069-2017.

Vecchi, G. A., and G. Villarini, 2014: Next season's hurricanes. **343 (6171)**, 618–619, https://doi.org/10.1126/science.1247759.

Vecchi, G. A., M. Zhao, H. Wang, G. Villarini, A. Rosati, A. Kumar, I. M. Held, and R. Gudgel, 2011: Statistical–dynamical predictions of seasonal north atlantic hurricane activity. *Monthly Weather Review*, **139 (4)**, 1071–1087, https://doi.org/10.1175/2010MWR3499.1.

Vecchi, G. A., and Coauthors, 2014: On the seasonal forecasting of regional tropical cyclone activity. *Journal of Climate*, **27 (21)**, 8065–8087, https://doi.org/10.1175/JCLI-D-14-00158.1.

Vecchi, G. A., and Coauthors, 2019: Tropical cyclone sensitivities to co2 doubling: roles of atmospheric resolution, synoptic variability and background climate changes. *Climate Dynamics*, **53 (9)**, 5999–6033, https://doi.org/10.1007/s00382-019-04913-y.

Villarini, G., B. Luitel, G. A. Vecchi, and J. Ghosh, 2019: Multi-model ensemble forecasting of north atlantic tropical cyclone activity. *Climate Dynamics*, **53**, 7461–7477, https://doi.org/10.1007/s00382-016-3369-z.

Villarini, G., G. A. Vecchi, T. R. Knutson, and J. A. Smith, 2011: Is the recorded increase in short-duration north atlantic tropical storms spurious? *Journal of Geophysical Research: Atmospheres*, **116**, D10 112, https://doi.org/10.1029/2010JD015493.

Villarini, G., G. A. Vecchi, and J. A. Smith, 2010: Modeling the dependence of tropical storm counts in the north atlantic basin on climate indices. *Monthly Weather Review*, **138 (7)**, 2681–2705, https://doi.org/10.1175/2010MWR3315.1.

Villarini, G., G. A. Vecchi, and J. A. Smith, 2012: U.s. landfalling and north atlantic hurricanes: Statistical modeling of their frequencies and ratios. *Monthly Weather Review*, **140 (1)**, 44–65, https://doi.org/10.1175/MWR-D-11-00063.1.

Watt-Meyer, O., and Coauthors, 2025: ACE2: Accurately learning subseasonal to decadal atmospheric variability and forced responses. *npj Climate and Atmospheric Science*, **8 (1)**, 205, https://doi.org/10.1038/s41612-025-01090-0.

Yang, W., T.-L. Hsieh, and G. A. Vecchi, 2021: Hurricane annual cycle controlled by both seeds and genesis probability. *Proceedings of the National Academy of Sciences*, **118 (41)**, e2108397 118, https://doi.org/10.1073/pnas.2108397118.

Young, R., and S. Hsiang, 2024: Mortality caused by tropical cyclones in the united states. **635 (8037)**, 121–128, https://doi.org/10.1038/s41586-024-07945-5.

Zhang, G., M. Rao, J. Yuval, and M. Zhao, 2025: Advancing seasonal prediction of tropical cyclone activity with a hybrid ai–physics climate model. *Environmental Research Letters*, **20 (9)**, 094 031, https://doi.org/10.1088/1748-9326/adf864.

Zhao, M., I. M. Held, S.-J. Lin, and G. A. Vecchi, 2009: Simulations of global hurricane climatology, interannual variability, and response to global warming using a 50-km resolution gcm. *Journal of Climate*, **22 (24)**, 6653–6678, https://doi.org/10.1175/2009JCLI3049.1.

Zhao, M., I. M. Held, and G. A. Vecchi, 2010: Retrospective forecasts of the hurricane season using a global atmospheric model assuming persistence of sst anomalies. *Monthly Weather Review*, **138 (10)**, 3658–3675, https://doi.org/10.1175/2010MWR3366.1.